Eccentric Compression Performance of Parallel Bamboo Strand Lumber Columns

Hai-tao Li,[a,*] Jing-wen Su,[a] Andrew John Deeks,[b,*] Qi-sheng Zhang, [a] Dong-dong Wei, [c] and Cong-gan Yuan [c]

The influence of eccentricity ratio on the behaviour of 50 parallel bamboo strand lumber (PBSL) column specimens was studied under eccentric compression. The load-strain and load-deflection relationships were obtained from column tests, and the detailed failure modes for all specimens are reported. The eccentricity ratio is the main influencing factor on the bearing capacity of the columns, and the ultimate load values decreased with an increase of the eccentricity ratio. Both the ultimate middle deflection values and the absolute ultimate longitudinal strain values initially increased with the increase of the eccentricity ratio, and then stabilized or decreased slightly when the eccentricity ratio was bigger than approximately 0.8. The absolute ultimate lateral strain values for both face A (bracket side or compression side) and face C (tension side) performed similarly with the increasing of eccentricity ratios, increasing initially and then stabilizing or decreasing slowly. An equation for calculating the eccentricity influencing coefficient of PBSL columns is proposed. The calculation results obtained from the equations agreed well with the test results.

Keywords: Parallel bamboo strand lumber column; Eccentricity ratio; Deflection; Ultimate load

Contact information: a: College of Civil Engineering, Nanjing Forestry University, Nanjing 210037, China; b: College of Engineering and Architecture, University College Dublin, Dublin, Ireland; c: Jiangxi Feiyu Bamboo product Co., LTD, Fengxin 330700, China;
** Corresponding author: lhaitao1982@126.com; andrew.deeks@ucd.ie*

INTRODUCTION

Due to its excellent mechanical performance, high efficiency, ease of procurement, and environmental friendliness, bamboo has attracted significant attention in terms of its potential to be used in the construction industry as a sustainable construction material. To support the potential use of bamboo in construction, various attempts have been made to explore the mechanical behavior of bamboo (Amada *et al*. 1997; Yu *et al*. 2003; Varela *et al*. 2010; Malanit *et al*. 2011; Mahdavi *et al*. 2011; Verma and Chariar 2012; Li *et al*. 2013, 2015; Gottron *et al*. 2014; Liu *et al*. 2014; Xu *et al*. 2014; Sinha *et al*. 2014; Su *et al*. 2015a; Richard and Harries 2015).

The use of unprocessed bamboo in construction is limited by the relatively small diameter of the bamboo culm and the low rigidity of the bamboo material. To enhance dimensional consistency, strength, and uniformity, and to solve the limitation of member size, the bamboo culm can be disassembled into bamboo filament bundles by passing it through a roller press crusher and then gluing it together with adhesive to form certifiable structural members. The composite material is called parallel bamboo strand lumber (PBSL) (Huang 2009; Ahmad and Kamke *et al*. 2011; Su *et al*. 2015b).

Huang (2009) studied the aging resistant performance of parallel bamboo strand lumber in three aspects, including the basic material performance of PBSL. Cheng (2009) investigated the effect on performance of bamboo bundle preparation, glue immersion, and the forming and hot pressing process adopting manufacturing processes used elsewhere for reconstituted lumber, endeavoring to utilize the entirety of bamboo through improved equipment and development of new technology. Pannipa *et al*. (2011) demonstrated that the resin type has a significant effect on board properties through an experimental study.

Naresworo and Ando (2000; 2001) conducted a study to determine the suitability of zephyr strands from moso bamboo (*Phyllostachys pubescens* Mazel) for structural composite board manufacture. Ahmad and Kamke (2011) analyzed the physical and mechanical properties of parallel strand lumber (PSL) made from Calcutta bamboo, which showed the suitability of Calcutta bamboo as a raw material for structural composite products. Cui *et al*. (2012) investigated the flexural characteristics of parallel strand lumber (PSL). A recent study by Wei *et al*. (2012) examined the failure of bamboo scrimber beams in detail, and concluded that the cross-sectional stiffness was the control condition for design load. Su *et al*. (2015b) investigated the mechanical performance of PBSL columns under axial compression. Li *et al*. (2015) carried out a preliminary investigation of PBSL under axial compression for different directions based on large-scale specimens and also discussed the experimental study and analysis on parallel bamboo strand lumber column under eccentric compression preliminarily; however the number of test specimens was just 8, and many properties have not been investigated.

To the authors' knowledge, most of the previous studies on parallel bamboo strand lumber in compression have been conducted under axial compression conditions. However, almost all columns used are under eccentric compression in the building industry. Few studies have been performed under eccentric compression both for wood and for bamboo lumber pieces. As the shear stress is weak for these two kinds of materials and the strict requirement for the test setup, it is difficult to perform the eccentric compression test. The behaviour of structural members under eccentric compression could be significantly different from its behaviour under axial compression. This study aims to examine the eccentric compression behaviour of PBSL structural members and investigate how the eccentricity ratio influences the behavior of PBSL columns under eccentric compression.

To achieve these objectives, the study examines in detail the behaviour of full size structural members (with a design cross section of 100 mm x 100 mm) constructed from parallel bamboo strand lumber (PBSL) with different eccentricity ratios. Based on the test study and analysis, the formula for calculating the eccentricity influencing coefficient factors will be proposed for the columns.

EXPERIMENTAL

Materials

Moso bamboo (*Phyllostachys pubescens* from Feng-xin county in Jiang-xi province), was harvested at the age of 3 to 4 years. Bamboo strips from the upper growth of a 2000 mm tall culm were selected. The culms cut from the assigned growth portions were then split into 20 mm wide strips, and the outer skin (epidermal) and inner cavity layer (pith peripheral) were removed using a planer. All culm strips were split into bamboo filament bundles by passing through a roller press crusher. These bamboo filament bundles

were then dried and charred at a temperature of 165 °C and an air pressure of 0.3 MPa. Finally the bundles (Fig. 1) were made into PBSL by Fei-yu Co. Ltd.

Fig. 1. Original bamboo strand bundles

Fig. 2. Molds for parallel bamboo strand lumber

Phenolic glue (Danning 4I glue with 43.2% solids content, pH=9.1 and 70 MPa.s viscosity) was used to manufacture the parallel bamboo strand lumber specimens. All bundles were put into molds (Fig. 2), and these were then were pressed together to form blocks. A transverse compression of 90 MPa was applied for the blocks under the normal pressing temperature and then all the blocks were cured at 140 °C. The final moisture content was 8.22%, and the density was 1018 kg/m^3 for the laminate sourced from the upper portion. According to the compression tests for the specimens with dimensions of 100 mm× 100 mm× 300 mm, the compression strength for the parallel bamboo strand lumber was 64.6 MPa with a modulus of elasticity of 11028 MPa, ultimate compression strain of 0.02, and a Poisson's ratio of 0.35.

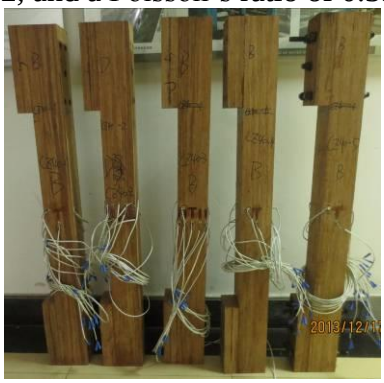

(a) Specimens

(b) Cross-section

Fig. 3. Structural charred parallel bamboo strand lumber

With the same cross-section of 100 mm× 100 mm and same length of 1200 mm, 10 groups of specimens were constructed. The designed eccentricity values are 0 mm, 10 mm, 25 mm, 40 mm, 55 mm, 70 mm, 80 mm, 90 mm, 100 mm, 120 mm, respectively. Each group consisted of five identical specimens (Fig. 3a) and the total number are 50 for the specimens. In addition, the specimen are named by 'CZ+ eccentricity'. The column end (with the bracket) cross-sectional structure of the PBSL can be seen in Fig. 3b.

Test Methods

The test arrangement is illustrated in Fig. 4. The displacement for the quarter points, including the mid-span deflection, was measured using three laser displacement sensors

(LDS type: Keyence IL-300, Japan). Two strain gauges were pasted on each middle side surface of the specimens, except for one side's surface (Face D) with six train gauges. The strain gauges were numbered as shown in Fig. 5. The load was along the eccentricity line, which is parallel to the axial line. The test was performed using a microcomputer-controlled electro-hydraulic servo universal testing machine (Sans Company, China, Fig. 6) with a capacity of 1000 kN, and an LDS data acquisition system.

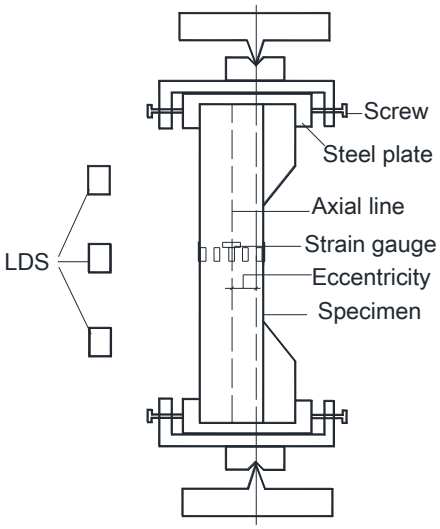

Fig. 4. Test scheme

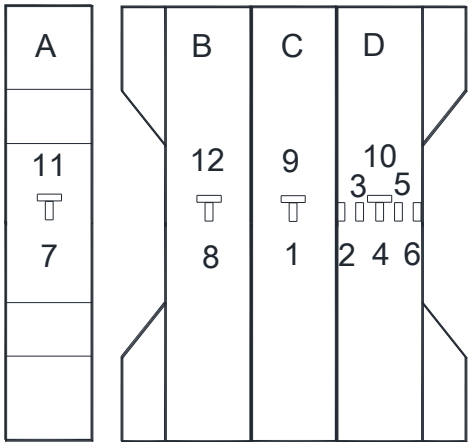

Fig. 5. Side surfaces

Fig. 6. Experiment for column specimen

Tests were conducted according to the standard for test methods of timber structures (GB/T 50329-2012) (2012). The load was initially applied through load control in the elastic stage, and then was changed to displacement control before the proportional limit. The test was continued at a certain displacement rate until the middle deflection value was about 40 mm after the peak load point, or the specimen had sustained significant damage, at which time testing was halted.

RESULTS AND DISCUSSION

Failure Modes and Mechanism Analysis

Typical failure modes can be seen in Fig. 7. Each specimen behaved elastically at the beginning of loading. With increased loading, the specimens showed a small amount of plastic deformation, and the stiffness of the column decreased significantly. As the deflection became obvious, cracks (accompanied by a slight noise) appeared on tensile surface C, where there were defects in areas such as the bamboo joints, mechanical connector parts, *etc*. Finally, the middle deflection value for the specimen increased about 40 mm or so after the peak load point was reached or the specimen had sustained significant damage before complete failure occurred and the columns shed most of the load. Except for face A, cracks can be seen clearly from the other three side surfaces. Bending failure occurred for the column specimens under eccentric compression.

(a) Face A

(b) Face B

(c) Face C

(d) Face D

Fig. 7. Failure photos for group CZ10-1

Typical load strain curves can be seen in Figs. 8 and 9. Figure 8 shows how eight longitudinal strains on the middle side surfaces change with the applied load for CZ10-3, while Fig. 9 shows the same plots for the lateral strains. All strains displayed an initial elastic phase. The ultimate longitudinal strain value on the compression surface of the specimen was the largest of the eight strains in Fig. 8, as is the ultimate lateral strain value on the compression surface among the four plotted in Fig. 9. The tensile failure always happened earlier than the compression failure for laminated bamboo. The main reason for this is that defects influenced the tensile strength more than compression strength.

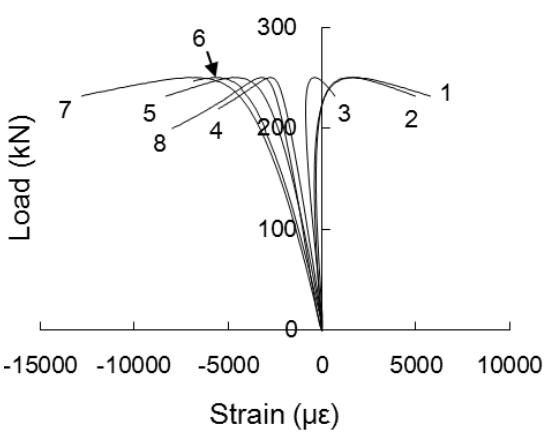

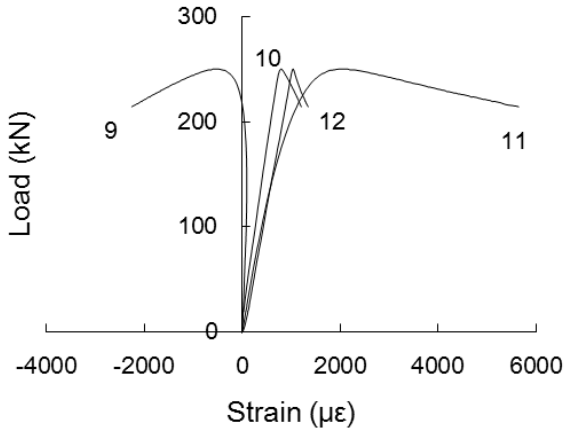

Fig. 8. Load-longitudinal strain curves for CZ10-3 **Fig. 9.** Load-lateral strain curves for CZ10-3

Figure 10 plots the typical lateral deflection curves under different load grades. Figure 10(a) shows how lateral deformation developed through different loading stages for the column with small eccentricity, while Fig. 10(a) shows corresponding results for the column with large eccentricity. The trends were similar for columns with both large and small eccentricity. Fitted sine half-wave curves were drawn using dotted lines in Fig. 10. It can be seen clearly that the measured deflections were close to the sine line no matter what the eccentricity was. The equation of the deflection curve can be expressed as (Eq. 1),

$$w = w_{\mathrm{m}} \sin \frac{\pi H}{L} \tag{1}$$

where w is the deflection of the PBSL column, w_{m} is the middle deflection value of the column, H is the height from the bottom to the calculation point of the column, and L is the total length of the column.

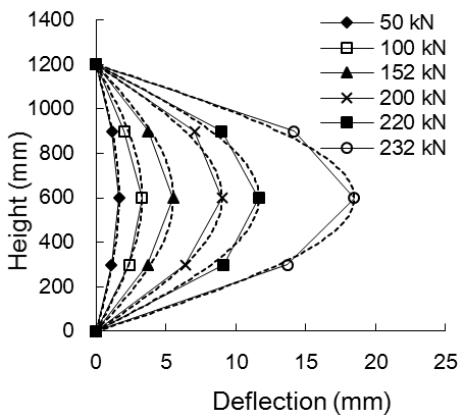

(a) Specimen CZ10-1

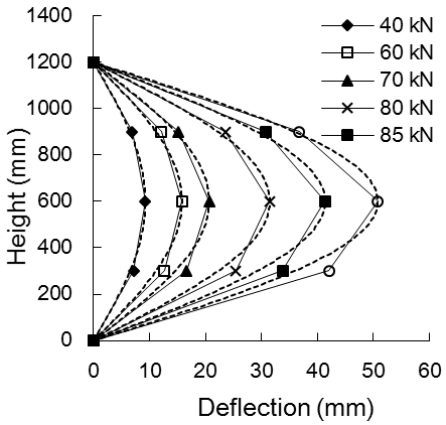

(b) Specimen CZ100-3

Fig. 10. Typical lateral deflection curves

Influence of Eccentricity on Strain Distribution

Figure 11 plots the evolution of the strain profile throughout loading for the mid-span cross-section of the two typical specimens. Each test showed that the strain across the cross-section of the laminated bamboo column was basically linear throughout the loading process, following standard normal section bending theory. However, over the course of

the loading process for the specimen with large eccentricity, the neutral axis moved downwards from the centre of the column, particularly during the latter part of the process. When the applied load reached the elastic limit, the fibres in the compression area entered the plastic state gradually, and the compression elastic modulus decreases, thus leading to internal force redistribution across the cross-section. Therefore, the neutral axis descended so as to achieve a new equilibrium position.

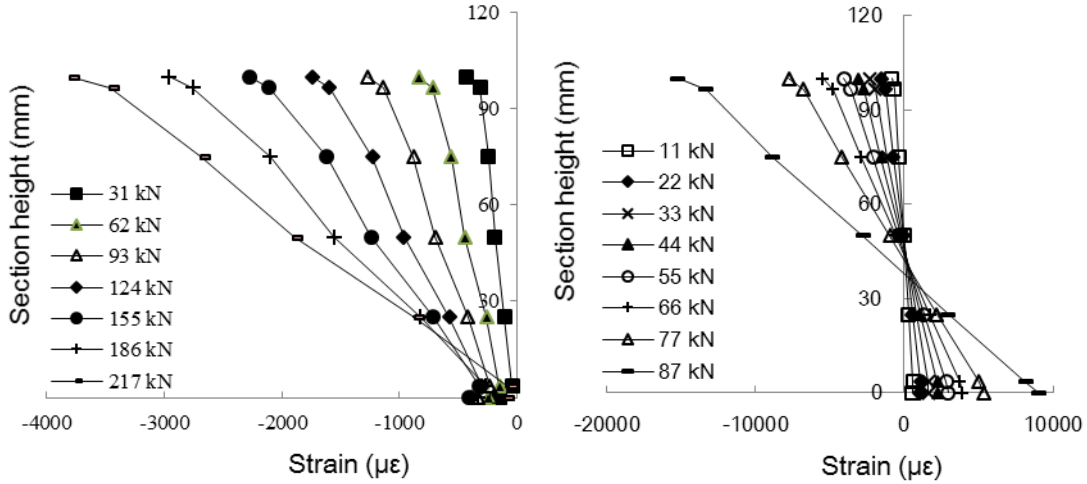

(a) Specimen CZ10-3 (b) Specimen CZ100-3

Fig. 11. Typical strain profile development for the mid-span cross-section

Influence of Eccentricity Ratio on Load and Deflection

Figure 12 plots the typical load against the middle deflection curves for the specimens with various eccentricity of load. The load and deflection curves show that these specimens were under elastic compression in the initial stage, followed by non-linear softening behaviour. After the peak load point, the lateral deflection increased quickly. The load decreased while the lateral deflection continued to increase until failure occurred. Purely plastic behaviour occurred specifically for the specimen with small eccentricity. As can be seen from Fig. 12, the rate at which the lateral deflection increases accelerated with the increase of eccentricity.

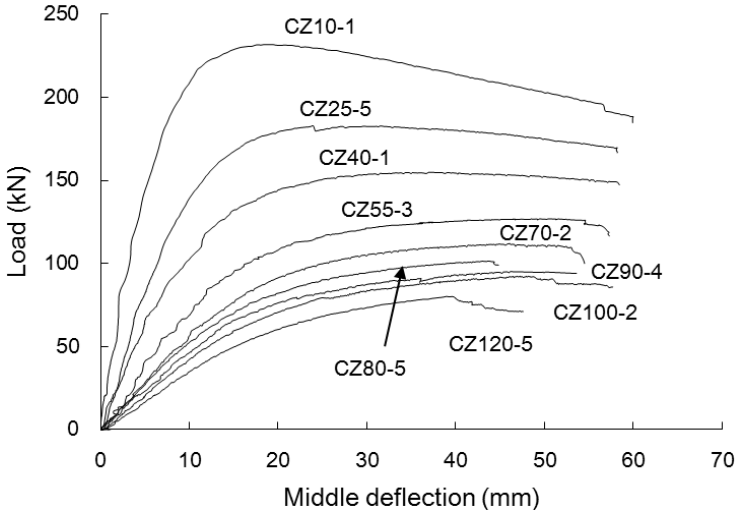

Fig. 12. Load-middle deflection curve comparisons for columns with different eccentricity

Deflection caused by initial defects influenced the bearing capacity of the specimens, increasing obviously as the eccentricity ratio was increased, and the larger the eccentricity ratio, the bigger the deflection corresponding with the peak load.

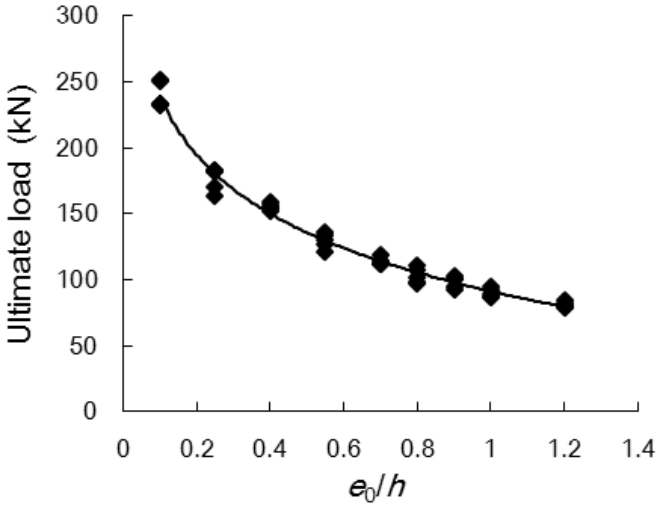

Fig. 13. Ultimate load comparison

Figure 13 plots the ultimate load comparison among different group specimens with different eccentricity ratios. The ultimate load values decreased with the increase of the eccentricity ratio. The eccentricity ratio was the main influencing factor on the bearing capacity of the columns. Using statistical regression from the test results, the relationship between ultimate load and eccentricity ratio, under the conditions mentioned previously, can be expressed as (Eq. 2),

$$N_{ul}=91.13-64.3\ln\left(e_0/h\right) \quad (2)$$

where N_{ul} is the ultimate bearing capacity of the PBSL column (kN), e_0 is the eccentricity value of the PBSL column (mm), and h is the height along the eccentric direction of the cross section (mm).

Figure 14 plots the middle deflection comparison against eccentricity ratios. As can be seen from Fig. 14, the ultimate middle deflection values initially increased with the increase of the eccentricity ratio, and then stabilized or decreased slightly when the eccentricity ratio was bigger than 0.8. The test data can be divided into three main stages. First, the ultimate middle deflection increased quickly when the eccentricity ratio was smaller than about 0.55, and then it increased slowly between the values 0.55 and 0.8. After that, the ultimate middle deflection values decreased slightly when the eccentricity ratio was bigger than 0.8. This means that there was a critical value after which the ultimate deflection did not change very much. Based on the test results, the value for this critical eccentricity ratio appears to be approximately 0.8. Utilizing statistical regression of the test results, the relationship between ultimate middle deflection and eccentricity ratio, under the conditions mentioned previously, can be expressed as (Eq. 3),

$$w_{ul}=96.63\left(e_0/h\right)-58.66\left(e_0/h\right)^2+7.88 \quad (3)$$

where w_{ul} is the ultimate middle deflection of the PBSL column (mm).

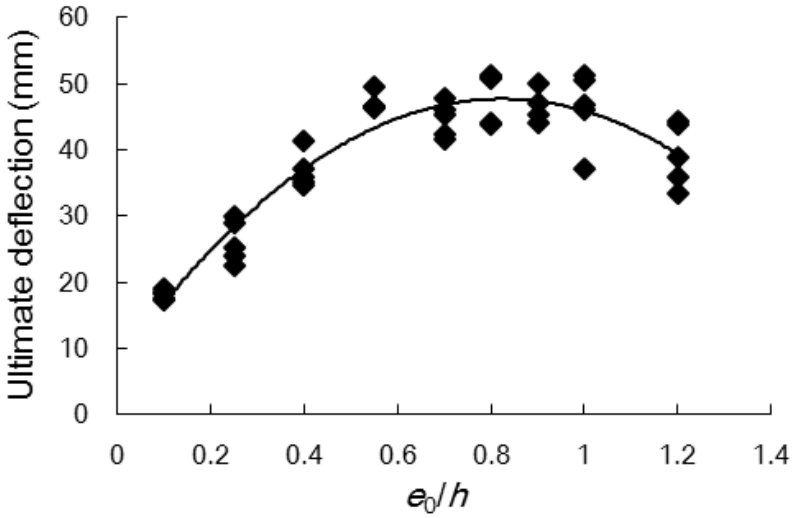

Fig. 14. Ultimate middle deflection comparison

As discussed above, the failure mode for columns under eccentric compression is similar to the failure mode for beams. The deflections at failure became larger with an increase of the eccentricity ratio, accompanied by decreasing of the bearing capacity.

Influence of Eccentricity Ratio on the Longitudinal Strain

Figure 15 plots the load against the longitudinal strain obtained from the mid-span cross-section of face A and face C for the test specimens with different eccentricity ratios. The longitudinal strains for face A were all negative, which means these faces were under compression, as shown in Fig. 15 (a). At the same time, all longitudinal strain values for face C were positive, except for specimen group CZ10 in Fig. 15 (b). When the load value was small, all four side surfaces for the specimens of group CZ10 were under compression, as the eccentricity was too small, resulting in minus values. The longitudinal strain for face C became positive after a certain load value, which is in accordance with the mechanical behavior characteristics of a column with small load eccentricity. Column specimens with a larger eccentricity ratio had higher ultimate longitudinal strain overall.

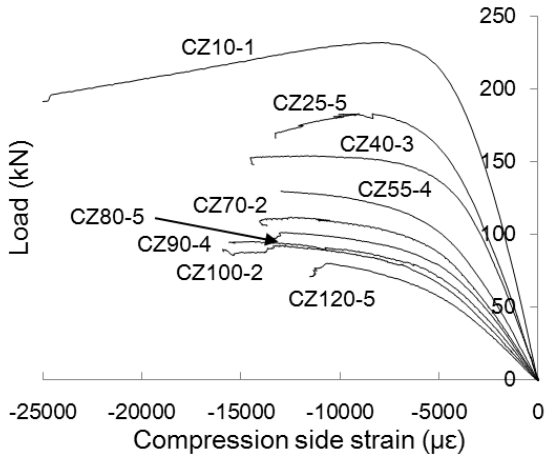

(a) Longitudinal strain for face A

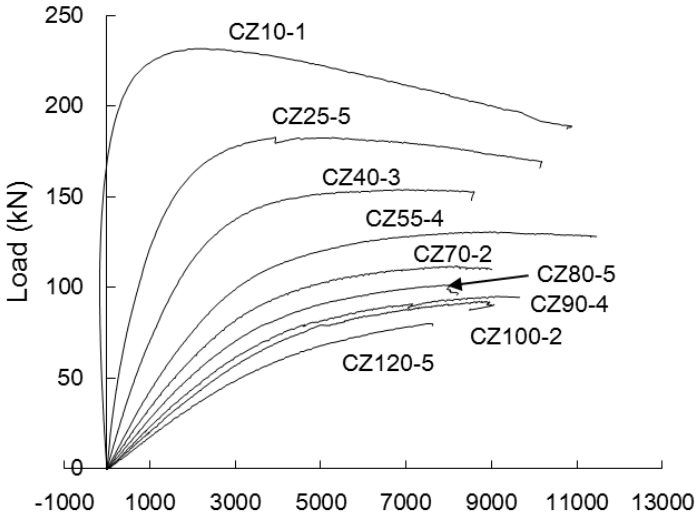

(b) Longitudinal strain for face C

Fig. 15. Typical load vs. longitudinal strain for the mid-span cross-section

Influence of Eccentricity Ratio on the Ultimate Strain

Figure 16 plots the ultimate strain against the eccentricity ratio for face A. As can be seen from these two figures, face A experienced compressive stress along the axial direction and tensile stress along the lateral direction. Both the absolute axial strain values and the lateral strain values were small for the column specimens with small eccentricity ratios, which means that the material strength had not been brought into full play when the specimen failed. These two kinds of strain initially increased with the increase of the eccentricity ratio, and then stabilized or decreased slightly when the eccentricity ratio was bigger than 0.8.

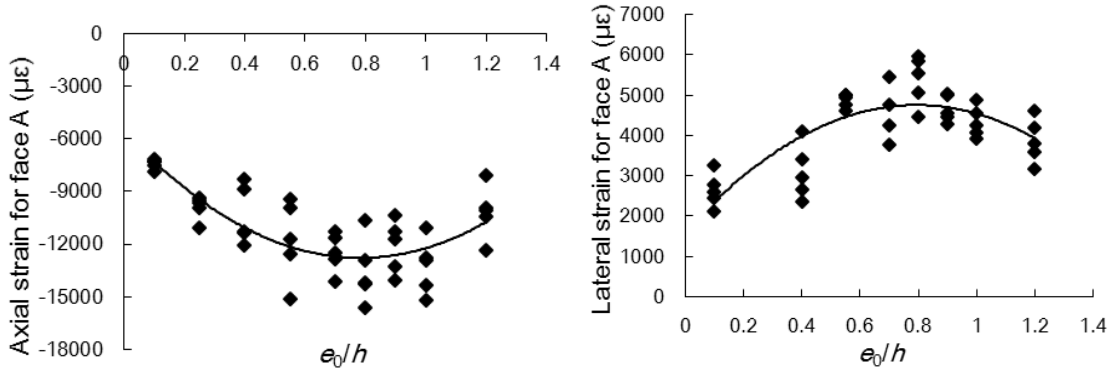

(a) Axial strain (b) Lateral strain

Fig. 16. Ultimate strain vs. eccentricity ratio (e_0/h) for face A

Using statistical regression from the test results, the relationship between ultimate strain and eccentricity ratio, under the conditions mentioned previously, can be expressed as

$$\varepsilon_{\text{uasA}} = 11731\left(e_0/h\right)^2 - 18372\left(e_0/h\right) - 5597 \quad (4)$$

$$\varepsilon_{\text{ulsA}}=7888\left(e_0/h\right)-4968\left(e_0/h\right)^2+1622 \quad (5)$$

where $\varepsilon_{\text{uasA}}$ is the ultimate axial strain for face A of the PBSL column ($\mu\varepsilon$), and $\varepsilon_{\text{ulsA}}$ is the ultimate lateral strain for face A of the PBSL column ($\mu\varepsilon$).

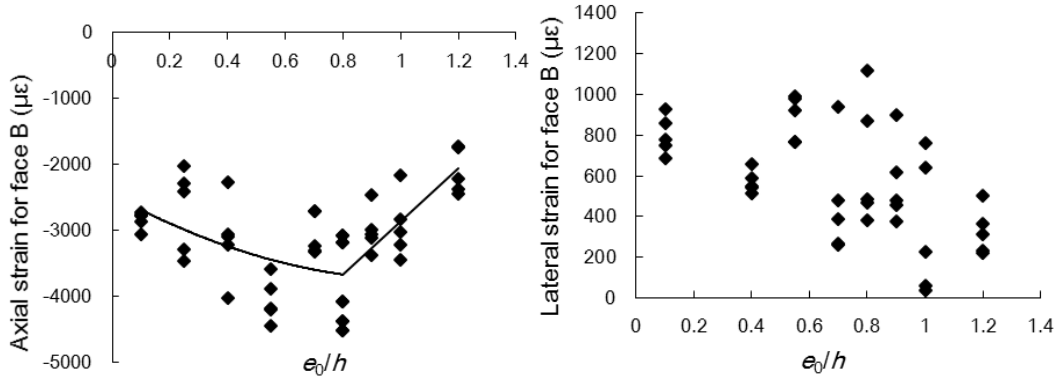

(a) Axial strain (b) Lateral strain

Fig. 17. Ultimate strain vs. eccentricity ratio (e_0/h) for face B

Figure 17 plots the ultimate strain against the eccentricity ratio for face B. Like face A, face B experienced compressive stress along the axial direction and tensile stress along the lateral direction. Both the absolute axial strain values and the lateral strain values were smaller than the corresponding values for face A. The absolute axial strain values increased clearly with the increasing of the eccentricity ratio initially, and then it decreased after the eccentricity ratio value exceeded approximately 0.8. However, the lateral strain values decreased at first, and then increased slowly as a whole with increasing eccentricity ratios. As the lateral strain values were very scattered, no equation is proposed here to represent this relationship. Using statistical regression from the test results, the relationship between ultimate axial strain and eccentricity ratio, under the conditions mentioned previously, can be expressed as,

$$\varepsilon_{\text{uasB}}=\begin{cases}1099\left(e_0/h\right)^2-2389\left(e_0/h\right)-2458 & e_0/h\le 0.8\\ 4018\left(e_0/h\right)-6885 & 0.8<e_0/h\end{cases} \quad (6)$$

where $\varepsilon_{\text{uasB}}$ is the ultimate axial strain for face B of the PBSL column ($\mu\varepsilon$).

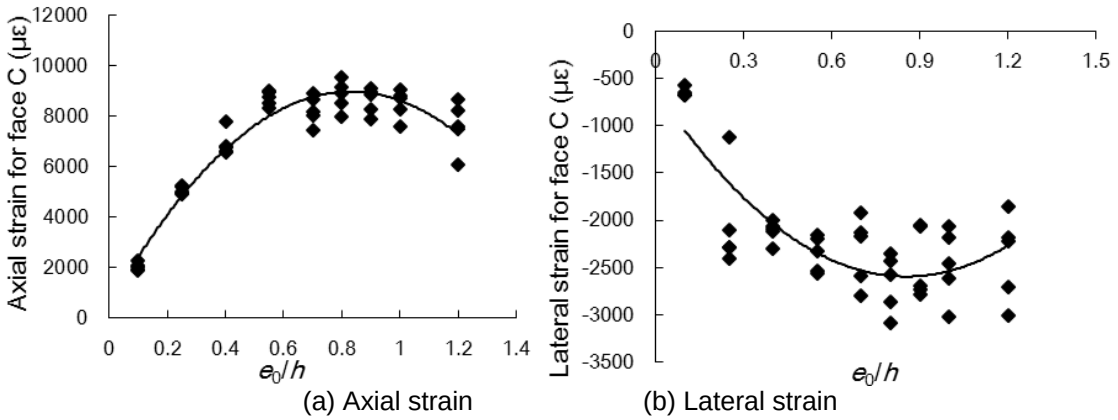

(a) Axial strain (b) Lateral strain

Fig. 18. Ultimate strain vs eccentricity ratio (e_0 / h) for face C

Figure 18 plots the ultimate strain against the eccentricity ratio for face C. As can be seen from these two figures, face C experienced tensile stress along the axial direction, and compressive stress along the lateral direction. There was something wrong with the strain gauges for group CZ25, and that is why there were no lateral strain values obtained from this group. Both the axial strain values and the absolute lateral strain values were small for the column specimens with small eccentricity ratios. Like face A, these two kinds of values increased clearly with increasing the eccentricity ratio initially, and then didn't change very much, or decreased slowly, after an approximately 0.8 eccentricity ratio value. The relationship between the ultimate strain and the eccentricity ratio was in agreement with the relationship between the ultimate middle deflection and the eccentricity ratio. Using statistical regression from the test results, the relationship between ultimate strain and eccentricity ratio, under these conditions, can be expressed as (Eqs. 7 and 8),

$$\varepsilon_{\text{uasC}} = -12236\left(e_0 / h\right)^2 - 20331\left(e_0 / h\right) - 518 \quad (7)$$

$$\varepsilon_{\text{ulsC}} = 2721\left(e_0 / h\right)^2 - 4643\left(e_0 / h\right) - 615 \quad (8)$$

where $\varepsilon_{\text{uasC}}$ is the ultimate axial strain for face C of the PBSL column (με), and $\varepsilon_{\text{ulsC}}$ is the ultimate lateral strain for face C of the PBSL column (με).

Combined Results

The eccentricity influence coefficient (φ_e) for calculating the ultimate bearing capacity can be expressed as (Eq. 9),

$$\varphi_e = N_{\text{ul}} / N_0 \quad (9)$$

where N_{ul} is the ultimate bearing capacity of PBSL columns under eccentric compression, and N_0 is the ultimate bearing capacity of PBSL columns under axial compression.

In reality, there is an interaction between the eccentricity influence coefficient and geometric parameters of the PBSL columns. Combining with the numerical analysis and then reevaluating the constant coefficients by statistical regression on the whole test data set, an equation for calculating the eccentricity influence coefficient φ_e of PBSL columns can be expressed as (Eq. 10),

$$\varphi_e = \frac{1}{1.685 + 3.459 e_0 / h} \quad (10)$$

where e_0 is the eccentricity value of the PBSL column, and h is the height along the eccentric direction of the cross section.

According to formula (9), the ultimate bearing capacity can be calculated using the following equation (Eq. 11),

$$N_{ul} = \varphi_e N_0 \quad (11)$$

where the stability coefficient φ_e can be calculated by Eq. 10.

Table 1 compares the test results with the calculation results using Eq. 11. N_u^t is the ultimate test load, and N_u^e is the calculated ultimate load using Eq. 10. The symbol μ stands for the average value of N_u^t/N_u^e. It can be seen clearly that the standard deviation coefficients for most of the groups were less than 0.05, except for one group with an eccentricity value of 80 mm. The standard deviation coefficient for group CZ80 was 0.058, which is also not very big. In addition, most of the coefficients of variation were less than 0.051, except for group CZ80 with a value of 0.059. As a whole, all of these standard deviations and coefficients of variation were small. That is to say, the calculation results obtained from the equation agreed well with the test results.

Table 1. Comparison Between the Test Results and Calculation Results

Group	Eccentricity ratio e_0 / h	Eccentricity influencing coefficient φ_e	Test results N_u^t (kN)	Calculation results N_u^c (kN)	Average value μ	Standard deviation	Coefficients of variation
CZ10	0.1	0.492	240.1	229.9	1.044	0.043	0.041
CZ25	0.25	0.392	176.4	183.1	0.963	0.049	0.051
CZ40	0.4	0.326	155.2	152.1	1.021	0.017	0.017
CZ55	0.55	0.279	129.7	130.1	0.997	0.047	0.047
CZ70	0.7	0.244	113.9	113.7	1.002	0.027	0.027
CZ80	0.8	0.225	102.9	104.9	0.982	0.058	0.059
CZ90	0.9	0.208	98.15	97.3.	1.009	0.042	0.041
CZ100	1	0.194	90.09	90.75	0.993	0.040	0.040
CZ120	1.2	0.171	81.01	79.99	1.013	0.027	0.027

CONCLUSIONS

1. The eccentricity ratio of the load was the main influencing factor affecting the bearing capacity of the columns. The ultimate load values decreased with the increase of the eccentricity ratio.
2. Both the ultimate middle deflection values and the absolute ultimate longitudinal strain initially increase with the increase of the eccentricity ratio, and then stabilize or decrease slightly when the eccentricity ratio is bigger than approximately 0.8.

3. The absolute ultimate lateral strain values for both face A and face C behaved similarly with increases of the eccentricity ratio, increasing initially, and then stabilizing, or decreasing slowly. However, the ultimate lateral strain values for face B decreased first, and then generally increase slowly with increases of the eccentricity ratio.

4. An equation for calculating the eccentricity influence coefficient (φ_e) of parallel bamboo strand lumber columns was proposed. The calculation results obtained from the equations agreed well with the test results.

ACKNOWLEDGMENTS

The material presented in this paper is based upon work supported by the National Natural Science Foundation of China (51308301), the Foundation of the Doctoral Program of the Ministry of Education under Grant No. 20123204120012, the Natural Science Foundation of Jiang-su Province (No. BK20130978), Jiangsu Postdoctoral Science Foundation Project (No. 1501037A), and a Project Funded by the Priority Academic Program Development of Jiangsu Higher Education Institutions. Any opinions, findings, conclusions, or recommendations expressed in this material are those of the writer(s), and do not necessarily reflect the views of the foundations. The writers gratefully acknowledge Nian-qiang Zhou, Qi-jun Wang, Zhuang-yan Shen, Hao Yang, Ming-lei Yao, Shuai-hong Zhang, Jin-yuan Wang, Zhi-hao Yin, Jin-xiu Sun, Wei-xu Zhu, and others from the Nanjing Forestry University for helping with the tests.

REFERENCES CITED

Ahmad, M., and Kamke, F. A. (2011). "Properties of parallel strand lumber from Calcutta bamboo (*Dendrocalamus strictus*)," *Wood Sci. Technol.* 45(1), 63-72. DOI: 10.1007/s00226-010-0308-8

Amada, S., Ichikawa, Y., Munekata, T., Nagase, Y., and Shimizu, K. (1997). "Fiber texture and mechanical graded structure of bamboo," *Composites Part B: Eng*. 28, 13–20. DOI: 10.1016/s1359-8368(96)00020-0

China Building Industry Press. (2012). "Standard for test methods of timber structures," (GB/T 50329-2012), Beijing, China.

Cheng, L. (2009). "Manufacturing technology of reconstituted bamboo lumber," Huhehaote, China. Master's Thesis, Inner Mongolia Agricultural University, Hohhot, China.

Cui, H., Guan, M., and Zhu, Y. (2012). "The flexural characteristics of prestressed bamboo slivers reinforced parallel strand lumber (PSL)," *Key Engineering Materials* 517, 96-100. DOI: 10.4028/www.scientific.net/kem.517.96

Gottron, J., Harries, K. A., and Xu, Q. (2014). "Creep behavior of bamboo," *Construction and Building Materials* 66, 79-88. DOI: 10.1016/j.conbuildmat.2014.05.024

Huang, X. (2009). "The study on accelerated aging method and aging resistant performance of parallel bamboo strand lumber," Master's Thesis, Nanjing Forestry University, Nanjing, China.

Li, H., Zhang, Q., Huang, D., and Deeks, A. J. (2013). "Compressive performance of laminated bamboo," *Composites Part B: Engineering* 54, 319-328. DOI:

10.1016/j.compositesb.2013.05.035
Li, H., Su, J., Zhang, Q., Deeks, A. J., and Hui, D. (2015). "Mechanical performance of laminated bamboo column under axial compression," *Composites Part B: Engineering* 79, 374-382. DOI: 10.1016/j.compositesb.2015.04.027
Li, H., Su, J., Zhang, Q., and Chen, G. (2015). "Experimental study on mechanical performance of side pressure laminated bamboo beam," *Journal of Building Structures* 36(3), 121-126.
Liu, H., Jiang, Z., Zhang, X., Liu, X., and Sun, Z. (2014). "Effect of fiber on tensile properties of Moso bamboo," *BioResources* 9(4), 6888-6898. DOI: 10.15376/biores.9.4.6888-6898
Li, H., Su, J., Wei, D., Zhang, Q., and Chen, G. (2015). "Comparison study on parallel bamboo strand lumber under axial compression for different directions based on the large scale, *Journal of Zhengzhou University (Engineering Science)* 36(5), 31-36.
Li, H., Su, J., Zhang, Q., Wei, D., and Chen, G. (2015). "Experimental study and analysis on parallel bamboo strand lumber column under eccentric compression," *Journal of Building Materials* (http://www.cnki.net/kcms/detail/31.1764.TU.20150313.1054.022.html).
Lu, T., Jiang, M., Hui, D., and Zhou, Z. (2013). "Effect of surface modification of bamboo cellulose fibers on mechanical properties of cellulose/epoxy composites," *Composites Part B: Eng*. 51, 28-34. DOI: 10.1016/j.compositesb.2013.02.031
Lu, T., Liu, S., Jiang, Man, Xu, X., Wang, Y., Wang, Z, Gou, J., Hui, D., and Zhou, Z. (2014). "Effects of modifications of bamboo cellulose fibers on the improved mechanical properties of cellulose reinforced poly(lactic acid) composites," *Composites Part B: Engineering* 62, 191-197. DOI: 10.1016/j.compositesb.2014.02.030
Mahdavi, M., Clouston, P. L., and Arwade, S. R. (2011). "Development of laminated bamboo lumber: Review of processing, performance, and economical considerations," *Journal of Materials in Civil Engineering* 23(7), 1036-1042. DOI: 10.1061/(asce)mt.1943-5533.0000253
Malanit, P., Barbu, M. C., and Frühwald, A. (2011). "Physical and mechanical properties of oriented strand lumber made from an Asian bamboo (*Dendrocalamus asper* Backer)," *European Journal of Wood and Wood Products* 69(1), 27-36. DOI: 10.1007/s00107-009-0394-1
Naresworo, N., and Ando, N. (2000). "Development of structural composite products made from bamboo I: Fundamental properties of bamboo zephyr board," *J. Wood Sci.* 46(1), 68-74. DOI: 10.1007/bf00779556
Naresworo, N., and Ando, N. (2001). "Development of structural composite products made from bamboo II: Fundamental properties of laminated bamboo lumber," *J. Wood Sci.* 47(3), 237-242. DOI: 10.1007/bf01171228
Richard, M. J., and Harries, K. A. (2015). "On inherent bending in tension tests of bamboo," *Wood Science and Technology* 49(1), 99-119. DOI: 10.1007/s00226-014-0681-9
Su, J., Li, H., Yang, P., Zhang, Q., and Chen, G. (2015a). "Mechanical performance study on laminated bamboo lumber column pier under axial compression," *China Forestry Science and Technology* 29(4), 45-49.
Su, J., Wu, F., Li, H., and Yang, P. (2015b). "Experimental research on parallel bamboo strand lumber column under axial compression," *China Science paper* 10(1), 39-41.

Sinha, A., Way, D., and Mlasko, S. (2014). "Structural performance of glued laminated bamboo beams," *Journal of Structural Engineering* 140(1), 04013021-1-8. DOI: 10.1061/(asce)st.1943-541x.0000807

Varela, S., Correal, J. F., Yamin, L., and Ramirez, F. (2010). "Adhesive bond performance in glue line shear and bending for glued laminated guadua bamboo," *Journal of Tropical Forest Science* 22(4), 433-439. DOI: 10.1061/(asce)st.1943-541x.0000758

Verma, C. S., and Chariar, V. M. (2012). "Development of layered laminate bamboo composite and their mechanical properties," *Composites Part B: Engineering* 43(3), 1063-1069. DOI: 10.1016/j.compositesb.2011.11.065

Xu, M., Wu, X., Liu, H., Sun, Z., Song, G., Zhang, X., and Zhao, S. (2014). "Mode I fracture toughness of tangential *Moso* bamboo," *BioResources* 9(2), 2026-2032. DOI: 10.15376/biores.9.2.2026-2032

Wei, Y., Wu, G., Zhang, Q., and Jiang, S. (2012). "Theoretical analysis and experimental test of full-scale bamboo scrimber flexural components," *Journal of Civil, Architectural & Environmental Engineering* 34, 140-145.

Yu, W. K., Chung, K. F., and Chan, S. L. (2003). "Column buckling of structural bamboo," *Engineering Structures* 25, 755-768. DOI: 10.1016/s0141-0296(02)00219-5

Article submitted: April 27, 2015; Peer review completed: July 20, 2015; Revised version received: August 6, 2015; Accepted: August 10, 2015; Published: September 2, 2015.
DOI: 10.15376/biores.10.4.7065-7080